Arch. Min. Sci. **67** (2022), 3, 401-422

Electronic version (in color) of this paper is available: http://mining.archives.pl

DOI: https://doi.org/10.24425/ams.2022.142407

EKIN KÖKEN[1*]

ASSESSMENT OF LOS ANGELES ABRASION VALUE (LAAV) AND MAGNESIUM SULPHATE SOUNDNESS (M_{wl}) OF ROCK AGGREGATES USING GENE EXPRESSION PROGRAMMING AND ARTIFICIAL NEURAL NETWORKS

It has been acknowledged that two important rock aggregate properties are the Los Angeles abrasion value (LAAV) and magnesium sulphate soundness (M_{wl}). However, the determination of these properties is relatively challenging due to special sampling requirements and tedious testing procedures. In this study, detailed laboratory studies were carried out to predict the LAAV and M_{wl} for 25 different rock types located in NW Turkey. For this purpose, mineralogical, physical, mechanical, and aggregate properties were determined for each rock type. Strong predictive models were established based on gene expression programming (GEP) and artificial neural network (ANN) methodologies. The performance of the proposed models was evaluated using several statistical indicators, and the statistical analysis results demonstrated that the ANN-based proposed models with the correlation of determination (R^2) value greater than 0.98 outperformed the other predictive models established in this study. Hence, the ANN-based predictive models can reliably be used to predict the LAAV and M_{wl} for the investigated rock types. In addition, the suitability of the investigated rock types for use in bituminous paving mixtures was also evaluated based on the ASTM D692/D692M standard. Accordingly, most of the investigated rock types can be used in bituminous paving mixtures. In conclusion, it can be claimed that the proposed predictive models with their explicit mathematical formulations are believed to save time and provide practical knowledge for evaluating the suitability of the rock aggregates in pavement engineering design studies in NW Turkey.

Keywords: Rock aggregate; Aggregate properties; Los Angeles abrasion loss; Magnesium sulphate soundness; Gene expression programming; Artificial neural network

1. Introduction

Due to the advances in the construction and building industry, the demand and supply for rock aggregates have increased considerably. In the USA, for instance, an estimated 364 million metric tons of crushed stone was produced and shipped for consumption in the fourth quarter

[1] ABDULLAH GUL UNIVERSITY, NANOTECHNOLOGY ENGINEERING DEPARTMENT, 38100, KAYSERI – TURKEY

* Corresponding author e-mail: ekin.koken@agu.edu.tr

of 2020 [1]. Determining aggregate properties in a fast and reliable way becomes more of an issue in addressing such aggregate types that are to be used in various engineering fields. Due to the intensive use of rock aggregates in concrete (70-85% by volume) and paving mixtures (93-98% by volume), the quality of rock aggregates is of considerable importance in determining their suitability for any specific engineering applications [2]. Hence, rock aggregate quality should be investigated elaborately from the point of their degradation since rock aggregates used in construction and highway projects must effectively transmit the surcharge loads [3].

Additionally, rock aggregates are occasionally placed on natural soil to serve as a surface course. Therefore, they must be resistant to breakdown under definite loading conditions. To ensure construction aggregates fit this purpose and meet the requirements of end-uses, it is essential to understand the geology of the resources, production processes, standards, and test methods used to evaluate their suitability [4]. It has been seen that the characteristics of rock aggregates (e.g., size, shape, gradation, density, water absorption, abrasion, and freezing-thawing resistance) influence the durability and behaviour of concrete and paving mixtures.

Among the above rock aggregate properties, the resistance of aggregates against abrasion and fragmentation is mainly measured through several testing methods such as Los Angeles abrasion (LAAV), Nordic ball mill (NBM), and Micro-Deval (MDE) tests [5-10]. Specific to the mechanical aggregate properties, the Los Angeles abrasion value (LAAV) is one of the most accepted and widely used parameters for quantifying the abrasion resistance of rocks [11]. Kahraman and Toraman [12] and Ajalloeian and Kamani [13] declared that implementing the LAA test is relatively simple; however, it is time-consuming and requires many intentionally graded samples. Therefore, several relationships have been proposed to predict the LAAV using different rock properties.

For instance, the point load strength (PLS), Schmidt hammer value (SHV), uniaxial compressive strength (UCS), aggregate crushing value (ACV), aggregate impact value (AIV), and impact strength index (ISI) has been utilised to predict the LAAV of several rock types [14-22]. In addition, machine learning methods such as artificial neural networks and K-nearest neighbours have also been applied to evaluate the LAAV [19,23].

Mechanical rock aggregate properties vary on several factors. As earlier studies have pointed out, the grain size and the grain size distribution are critical geological parameters for explaining the mechanical properties of aggregates derived from rock materials [24]. Röthlisberger et al. [25] showed that the LAAV increases with the percentage of non-cuboidal grains in the feeding material. Okonta [26] established statistical relationships to predict the LAAV based on the average aggregate size with different shape properties. Räisänen [27], Liu et. al. [28], and Stålheim [29] also investigated rock textural effects on the LAAV. Their results indicated that the increase in average grain size (d_{50}) decreases the abrasion resistance of several granitic rocks. The abrasion resistance of metamorphic rocks increases in parallel with their quartz content [30]. Ajalloeian and Kamani [13] found a remarkable relationship between the textural coefficient (TC) and the LAAV for carbonate rocks. Hofer and Bach [31] also introduced a statistical model to estimate the mechanical properties of some railway ballast materials. They concluded that the mechanical properties such as the LAAV depend significantly on the petrographic and geometric properties of the feeding material. In a recent study by Tunc and Alyamac [10], surface response methodology (RSM) was employed to estimate the concrete strength based on various water/cement ratios and aggregate types having different LAAV values.

Another important aggregate property is the soundness of aggregates, which practically gives information on freezing-thawing and salt crystallisation effects acting on rock materials.

Based on AASHTO T104 [32], soundness refers to aggregate durability under meteorological conditions and indicates the resistance to physical and chemical weathering of fine and coarse aggregates. From this perspective, the effects of freezing-thawing on rocks have been handled by direct and indirect testing methods. Within the direct testing method, freezing-thawing cabinets have been utilised for rock and soil samples as specified by TS EN 1367–1 [33] and ASTM D6035/6035M [34], respectively.

The magnesium sulphate soundness (M_{wl}), an accelerated weathering test, is another alternative to simulating the freezing-thawing effects based on the dislocation of rock-forming minerals and volume expansion of grains [32,35,36]. Compared to the direct testing method, soundness tests such as sodium sulphate or magnesium sulphate are considerably preferable in most engineering applications due to their practicability.

Relating to the various environmental features, salt and ice crystallisation results in physical and chemical degradation in the rock itself [37-39]. When excluding the chemical properties of the solution engaging in the rock, salt and ice crystallisation are associated with thermodynamic properties of rock-forming minerals, pore geometry, size and micro-fissure-related moisture susceptibility of release surfaces [40, 41].

The presence of water or other salty solutions makes the overall rock structure slowly disintegrate and decreases the rock strength properties in the progress time [42]. Consequently, the water-rock interaction directly depends upon porosity and degree of microfracture in/on the rock material. The more the porosity and microfracture, the more susceptible is the rock. For instance, porous limestones can suffer from rapid degradation due to freezing-thawing cycles [43]. In this regard, soundness tests are convenient in assessing rock durability in harsh environmental conditions with a view to porosity and microfracture effects under the domination of salty solutions. However, soundness tests have a long-lasting testing procedure (i.e., in practical applications, one cycle of magnesium sulphate soundness approximately takes two days, and for a complete examination, at least five cycles are mainly required, according to TS EN 1367–2 [35]. Herein, it is logical to suppose that practical approaches or empirical formulae focusing on the LAAV and M_{wl} would evaluate the rock aggregate quality from several aspects. Herein, Rogers et al. [44] emphasised the importance of M_{wl} for the evaluation of fine aggregates. Consequently, they found considerable relationships between Micro-Deval abrasion loss (M_{DE}, %) and M_{wl}. Similar correlations were also obtained by Jayawickrama et al. [43], Phillips [45], and Fowler et al. [46].

Thanks to such empirical models or relationships, practical theories have been postulated, making engineering geological judgments much easier. Based on road and pavement design studies, rock aggregate quality must be quickly evaluated through practical approaches. The empirical models to predict several aggregate properties also provide practical knowledge on quarry quality control processes.

Therefore, fast and reliable techniques are required to estimate the fundamental aggregate properties. In this study, several aggregate properties of 25 different rock types located NW Turkey were documented. Statistical and soft computing methods were employed to estimate the LAAV and Mwl of the investigated rocks. For this purpose, mineralogical, physical and mechanical aggregate properties were determined for each rock type in the laboratory studies. Several predictive models were established based on gene expression programming (GEP) and artificial neural network (ANN) methodologies. The established predictive models were then compared to one another based on several statistical indicators. Furthermore, the suitability of the investigated rock types for use in bituminous paving mixtures was also evaluated based on an ASTM standard.

2. Materials and methods

Representative rock blocks were obtained from several parts of NW Turkey (Fig. 1). The investigated rocks are divided into two different types in terms of their lithology. Sedimentary rocks are limestone, and dolomitic limestone, whereas igneous rocks are identified as andesite, basaltic andesite, basalt, dacite, granodiorite, diorite, granite, gabbro, and diabase.

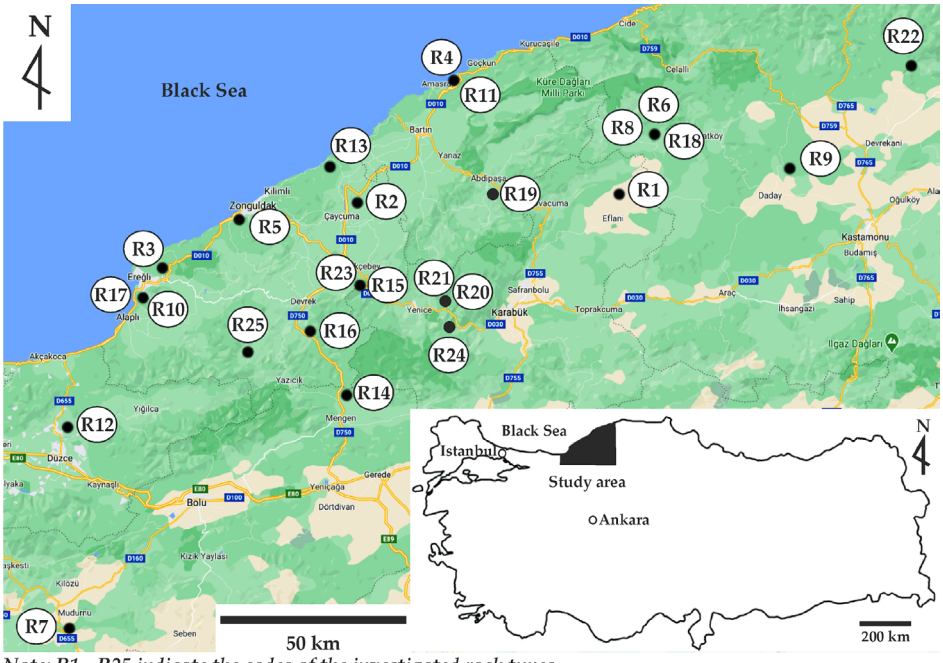

Note: R1 - R25 indicate the codes of the investigated rock types.

Fig. 1. Sampling locations of the rock blocks used in this study

In the laboratory studies, the mineralogical composition of the rocks was revealed using thin-section analyses. In addition, the dry unit weight (γ_d), water absorption by weight (w_a), and point load strength (PLS) were determined following the methods suggested by the International Society of Rock Mechanics [47]. Aggregate Impact Value (AIV), Los Angeles abrasion value (LAAV), Micro-Deval abrasion (M_{DE}), and magnesium sulphate soundness (M_{wl}) tests were carried out in accordance with BS 812–112 [48], TS EN 1097–2 [49], TS EN 1097–1 [50] and TS EN 1367–2 [35], respectively. The laboratory studies were performed under oven-dried conditions. Each laboratory test was repeated three times, and average values were presented in this research paper.

3. Laboratory studies

Laboratory studies were divided into three different stages. The first stage covers the determination of the mineralogical, physical, and mechanical properties of the rocks. Using a polarised

microscope, the rocks were characterised from the mineralogical point of view. For this purpose, thin sections were prepared for each rock type, and the quantities of rock-forming minerals were determined based on the point-counting method clearly defined by Larrea et al. [51]. For each rock type, at least three thin sections were analysed under a polarised microscope, and average quantities of rock-forming minerals were presented in this study.

Typical thin sections of the investigated rock are illustrated in Fig. 2. According to the thin section analysis results, it was determined that the mineralogical composition of the rocks is quite different due to the origins of the rock types. The mineralogical composition of the rocks is listed in Table 1. When focusing on Table 1, The calcite (cal) content of the limestones (R1-R12) varied from 74% to 95%. The andesitic rocks (R13-R17) had hyalopilitic and porphyritic textures,

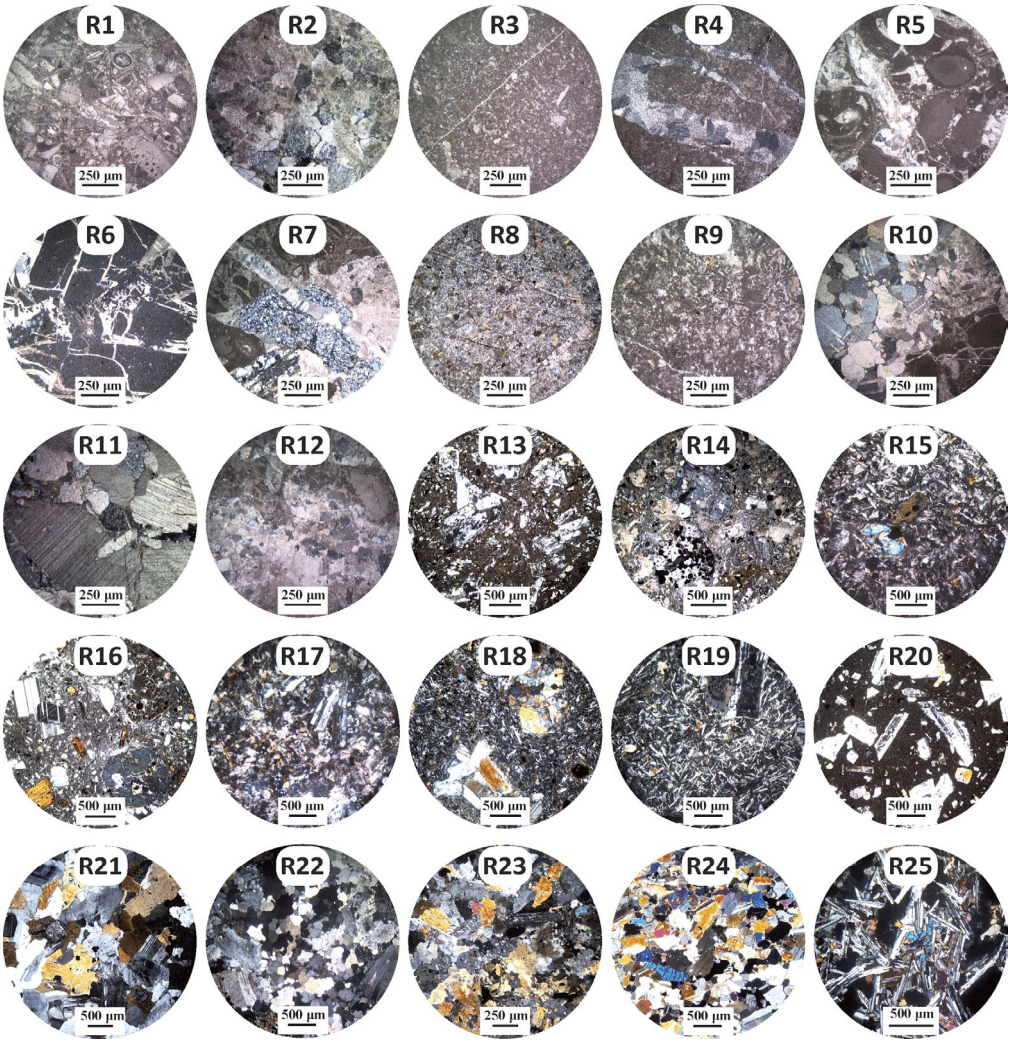

Fig. 2. Typical thin sections of the investigated rocks

TABLE 1

Mineralogical composition (areal percentage) for each rock type

Constituent (%)	Rock type												
	R1	R2	R3	R4	R5	R6	R7	R8	R9	R10	R11	R12	R13
Qtz.	–	–	–	–	–	–	–	–	–	–	–	–	–
Orth.	–	–	–	–	–	–	–	–	–	–	–	–	–
San	–	–	–	–	–	–	–	–	–	–	–	–	–
Plg.	–	–	–	–	–	–	–	–	–	–	–	–	61
Pryx.	–	–	–	–	–	–	–	–	–	–	–	–	1
Ol.	–	–	–	–	–	–	–	–	–	–	–	–	–
Horn.	–	–	–	–	–	–	–	–	–	–	–	–	1
Bt.	–	–	–	–	–	–	–	–	–	–	–	–	5
Mus.	–	–	–	–	–	–	–	–	–	–	–	–	–
Ep.	–	–	–	–	–	–	–	–	–	–	–	–	1
Chl.	–	–	–	–	–	–	–	–	–	–	–	–	1
Clay min.	–	–	–	–	–	–	–	–	–	–	–	–	7
Lim.	–	–	–	–	–	–	–	–	–	–	–	–	1
Sid.	–	–	–	1	1	1	1	3	2	–	–	1	–
Cal.	74	80	95	93	89	95	79	91	92	80	93	94	–
Dol.	–	11	1	4	–	1	2	1	–	18	6	5	–
Op. min.	1	1	3	1	–	1	2	4	1	1	1	–	6
Fossil rem.	25	8	1	1	10	2	16	1	5	1	–	–	–
Ground m.	–	–	–	–	–	–	–	–	–	–	–	–	16

Constituent (%)	Rock Type												
	R14	R15	R16	R17	R18	R19	R20	R21	R22	R23	R24	R25	
Qtz.	–	–	1	–	–	–	1	24	31	11	–	–	
Orth.	–	–	–	–	–	–	–	10	12	7	–	–	
San.	–	–	–	–	–	–	2	–	–	–	–	–	
Plg.	74	75	71	64	69	84	53	47	33	66	62	58	
Pryx.	2	3	4	5	12	5	–	6	7	6	16	14	
Ol.	–	–	–	–	1	–	–	–	–	–	3	1	
Horn.	–	1	3	18	2	1	–	7	5	4	4	10	
Bt.	3	3	3	2	1	1	1	4	5	2	2	7	
Mus.	–	–	–	–	–	–	1	–	1	1		–	
Ep.	1	1	1	–	1	1	2	1	–	1	1	2	
Chl.	1	–	1	–	–	–	–	–	1	–	–	2	
Clay min.	1	1	4	–	–	1	1	–	1	–	–	–	
Lim.	2	–	–	–	–	1	1	–	–	–	–	–	
Sid.	–	–	–	–	–	–	–	–	–	–	–	–	
Cal.	–	–	–	–	–	–	–	–	–	–	–	–	
Dol.	–	–	–	–	–	–	–	–	–	–	–	–	
Op. min.	9	6	4	6	6	2	1	1	4	2	12	2	
Fossil rem.	–	–	–	–	–	–	–	–	–	–	–	–	
Ground m.	7	10	8	5	8	4	37	–	–	–	–	4	

Explanations: Qtz: Quartz, Orth: Orthoclase San: Sanidine, Plg: Plagioclase, Ol: Olivine, Horn: Hornblende, Bt: Biotite, Mus: Muscovite, Ep: Epidote, Chl: Chlorite, Clay min: Clay minerals, Lim: Limonite, Sid: Siderite, Cal: Calcite (including micritic and sparitic) Dol: Dolomite, Fossil rem: Fossil remnant, Ground m: Ground mass.

whose plagioclase (plg) content was found to be between 61% and 65%. The basalts (R18, R19) had a porphyritic texture, and their pyroxene (prx) content varied from 5% to 12%. The dacitic rocks (R20) had an aphanitic texture and contained a considerable amount of groundmass. The granodiorite rocks (R21) had a phaneritic texture, whose quartz (qtz) content was about 24%. The granitic and dioritic rocks (R22, R23) had a granular texture and contained an orthoclase (orth) content ranging from 7% to 12%. Finally, the ultramafic rocks (R24, R25) were identified as gabbro and diabase, which has a large amount of plg content (58%-62%).

When it comes to the determination of physical and mechanical rock properties, the water absorption by weight (w_a), dry unit weight (γ_d), and point load strength (PLS) tests were involved. For this purpose, core samples with length to diameter ratio between 0.5-2.0 were prepared using an NX type (53.7 ± 0.5 mm) core drill, and rock saw.

The second and last stages of the laboratory studies deal with mechanical aggregate and soundness tests. For these tests, representative rock blocks were crushed using a laboratory-scale jaw crusher and sieved for specific size fractions (10-14 mm). After the sieving process, aggregates were washed using distilled water. Later on, they were placed in a drying oven at 105°C for 24 hours.

Before the LAAV and M_{wl} tests were performed, the degree of flakiness in the feeding material (FI) was also determined by BS EN 933–3 [52] (Table 2). To determine the FI for the specific size fraction of 10-14 mm, 6.3 and 5 mm bar sieves were used together and determined by the following equation (Eq. 1):

$$FI = \left(\frac{P_1 + P_2}{2W_1} \right) \times 100 \tag{1}$$

where P_1 and P_2 are the mass (g) of particles passing through the 6.3 and 5 mm bar sieves, respectively. W_1 is the total mass (g) of the feeding material tested.

TABLE 2

Apertures of bar sieves for flakiness index tests [52]

Particle size (mm)		Aperture of the bar sieve (mm)
12.5	16	8
10	12.5	6.3
8	10	5
6.3	8	4
5	6.3	3.15

Some of the laboratory studies are illustrated in Fig. 3. Based on the laboratory test results (Table 3), the PLS ranged from 3.79 to 12.96 MPa, while the AIV and LAAV were between 6.94-29.33% and 11.34-41.02%, respectively. Considering the PLS values in Table 3, the investigated rocks were identified from high strength to extremely high strength, according to Broch and Franklin [53]. Besides, when considering ASTM D692/692M [54] requirements, most of the investigated rocks were found to be suitable (LAAV ≤ 40% and M_{wl} ≤ 18%) for use in bituminous paving mixtures.

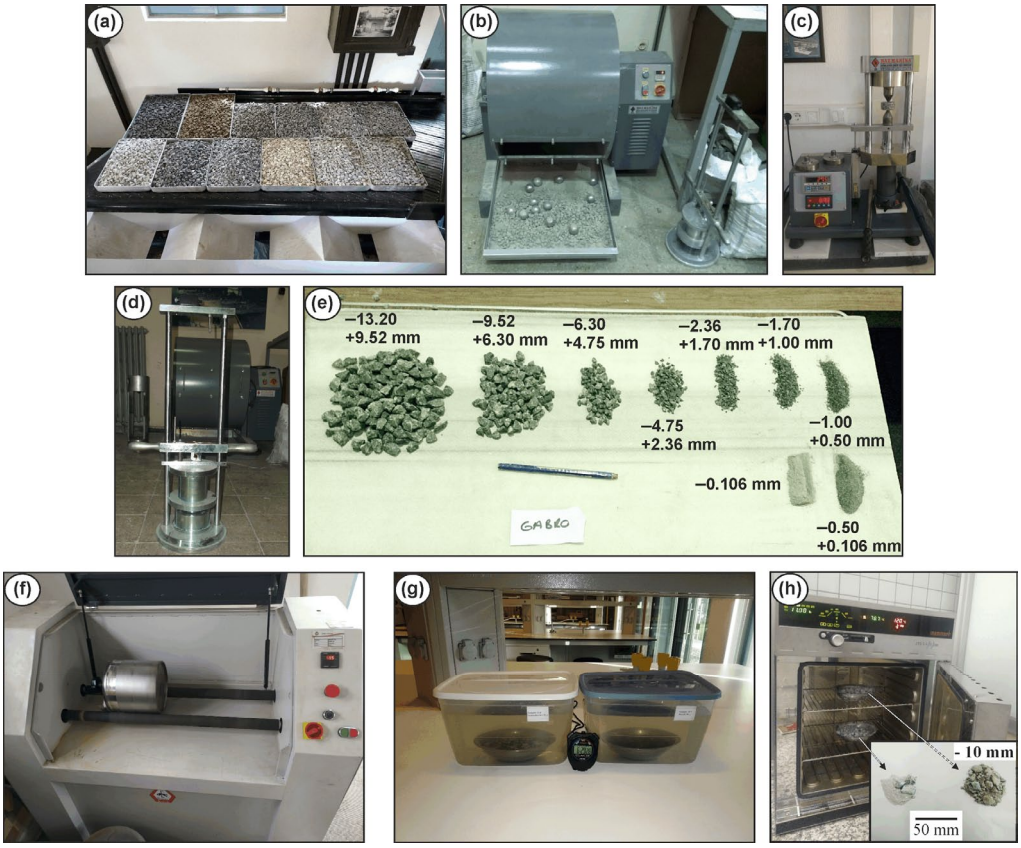

Fig. 3. Laboratory studies a) Some of the prepared rock aggregates b) LAA test c) PLS test d) AIV test device e) Crushed particles obtained from a single AIV test f) M_{DE} test g) M_{wl} test h) Drying process after some M_{wl} tests

TABLE 3

Laboratory test results

Rock type	Lithology	Location	γ_d (kN/m^3)	w_a (%)	PLS (MPa)	FI (%)	AIV (%)	LAAV (%)	M_{DE} (%)	M_{wl} (%)
1	2	3	4	5	6	7	8	9	10	11
R1	Limestone	Eflani /Karabuk	26.38	0.38	8.21	10.51	18.57	28.65	17.03	8.52
R2	Limestone	Caycuma /Zonguldak	25.53	0.45	6.75	6.48	22.21	22.96	14.02	7.01
R3	Limestone	Eregli /Zonguldak	25.81	0.64	6.08	8.17	17.41	31.11	12.68	3.94
R4	Limestone	Amasra /Bartin	25.75	0.50	8.46	16.45	17.59	25.30	17.83	9.69
R5	Limestone	Incivez /Zonguldak	25.42	0.78	8.86	11.63	19.09	29.77	17.05	3.39
R6	Limestone	Pınarbaşı /Kastamonu	25.99	1.24	3.95	10.52	21.58	28.45	15.88	8.64
R7	Limestone	Mudurnu /Bolu	24.42	2.50	5.74	14.14	29.33	41.02	28.38	20.19
R8	Limestone	Pınarbaşı /Kastamonu	26.09	0.41	7.32	9.30	18.54	25.27	16.28	2.74
R9	Limestone	Daday /Kastamonu	25.40	0.97	3.79	18.06	20.96	35.19	21.63	6.69

TABLE 3. Continued

1	2	3	4	5	6	7	8	9	10	11
R10	Dolomitic limestone	Eregli /Zonguldak	25.60	0.85	5.66	16.52	20.47	27.99	17.65	8.27
R11	Dolomitic limestone	Amasra /Bartin	26.55	0.31	8.30	11.48	16.20	24.03	11.93	4.69
R12	Dolomitic limestone	Akcakoca /Duzce	26.30	0.63	6.80	7.49	11.83	25.15	13.29	3.14
R13	Andesite	Filyos /Zonguldak	24.25	3.89	5.87	10.62	25.59	34.64	24.43	18.89
R14	Andesite	Mengen /Bolu	24.81	1.57	3.84	7.62	15.55	30.90	18.52	12.37
R15	Andesite	Gokcebey /Zonguldak	23.14	1.93	7.61	14.22	17.35	27.61	17.94	16.07
R16	Andesite	Devrek /Zonguldak	24.32	2.35	8.20	13.91	25.39	30.99	15.40	13.45
R17	Basaltic andesite	Eregli /Zonguldak	26.29	0.74	8.26	8.51	12.51	17.55	11.49	4.07
R18	Basalt	Pınarbaşı /Kastamonu	26.97	0.86	8.32	6.28	11.25	18.01	15.67	6.52
R19	Basalt	Abdipasa / Bartin	26.87	0.68	11.41	5.14	7.35	13.74	11.21	3.18
R20	Dacite	Karabuk / Yenice	25.31	1.33	10.60	10.44	13.44	24.00	11.89	8.26
R21	Granodiorite	Karabuk /Yenice	26.14	0.75	8.75	13.96	15.77	25.03	14.31	4.94
R22	Granite	Kure /Kastamonu	26.30	0.57	7.75	14.76	24.02	33.67	22.25	10.41
R23	Diorite	Gokcebey/ Zonguldak	27.66	0.54	9.52	6.58	16.40	21.87	15.11	4.05
R24	Gabbro	Yenice /Karabuk	28.24	0.17	12.96	14.25	6.94	15.45	10.90	3.58
R25	Diabase	Eğerci /Zonguldak	27.28	0.20	12.91	9.77	7.55	11.34	11.73	1.89

γ_d: Dry unit weight, w_a: Water absorption by weight, PLS: Point load strength, FI: Flakiness index, AIV: Aggregate impact value, LAAV: Los Angeles abrasion value, M_{DE}: Micro-deval abrasion value, M_{wl}: Magnesium sulphate soundness

4. Results and Discussion

4.1. Regression analyses

In this section, regression analyses were first carried out to achieve simple relationships for evaluating the LAAV and M_{wl}. Statistically meaningful single relationships to predict LAAV and M_{wl} are given in Fig 4. Accordingly, the maximum coefficient of determination (R^2) was found to be 0.76 and 0.73 for the LAAV and M_{wl}, respectively. Herein, the AIV is responsible for LAAV, whereas the w_a is associated with the M_{wl}. The M_{DE} is also associated with the LAAV and M_{wl} to some extent.

For the prediction of LAAV, similar linear models as a function of PLS and AIV were proposed by several researchers (Table 4). Apart from the linear relationships, logarithmic and exponential ones, as a function of AIV and PLI, were also reported by Kahraman and Gunaydin [14], Ozcelik [16], Ahmad et. al. [23], and Rigopoulos et. al. [55]. From evaluating M_{wl}, it can be possible to claim that the M_{wl} is associated with the w_a and M_{DE} for several rock types (Table 5). However, the relationship between these rock aggregate properties is not high enough for precise estimations. Therefore, it is required to have more reliable techniques to predict the M_{wl} with higher accuracy. To fulfil this aim, soft computing methods were employed, some of which

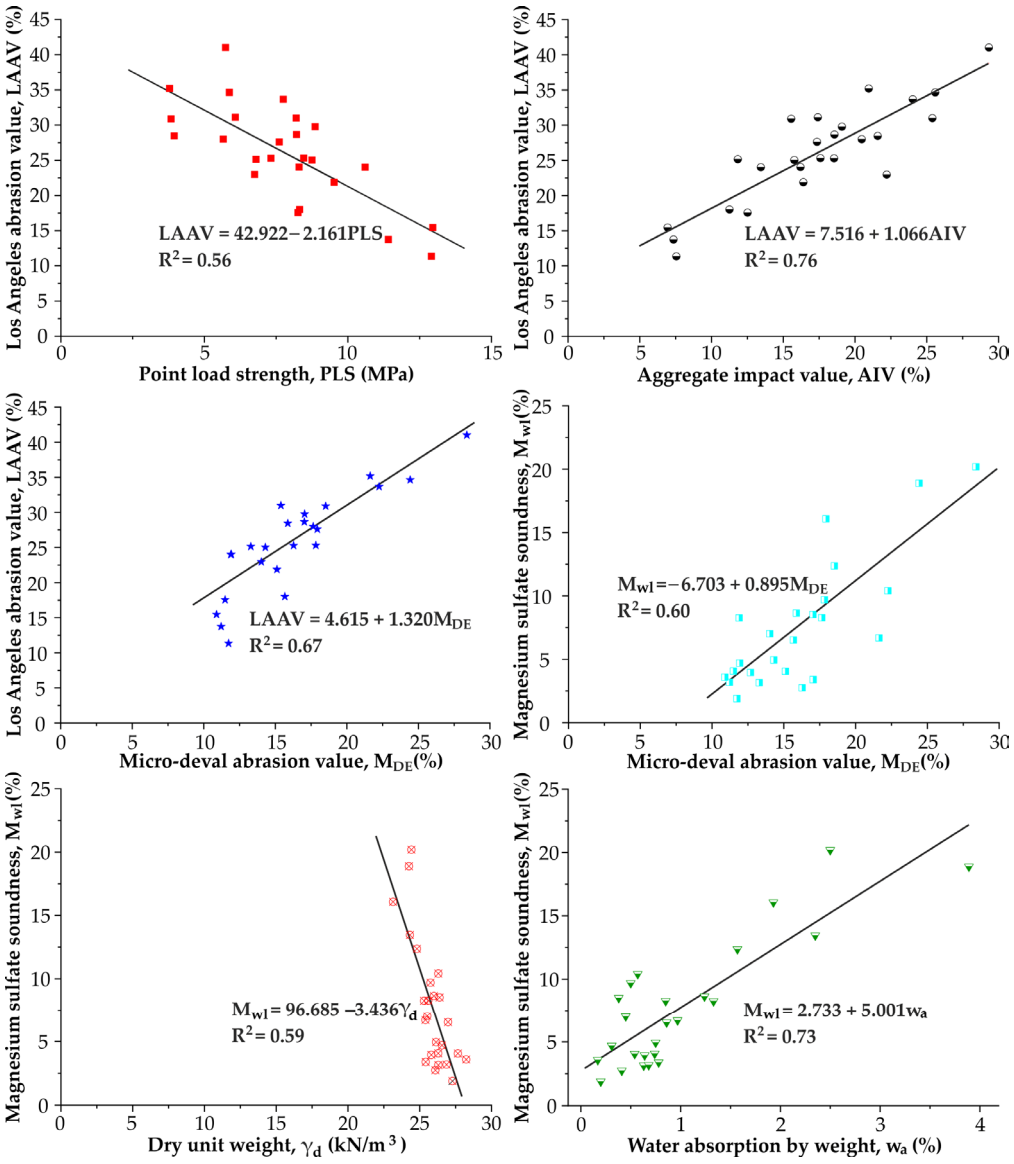

Fig. 4. Relationships to predict the LAAV and M_{wl}

are presented in the following section. However, it should be mentioned that several researchers [56-59] adopted and emphasised the LAAV test for evaluating the aggregate quality from several geological engineering aspects.

In this manner, it can be claimed that the LAAV reflects the mechanical quality of rock aggregates, whereas the M_{wl} can be of prime importance when assessing the resistance of rock aggregates against freezing-thawing and salt attacks.

TABLE 4

Empirical linear relationships to predict LAAV as a function of PLI and AIV

Equation	R^2	Number of samples in the analysis	Reference
$LAAV = 1.22AIV + 2.56$	0.82	110	[2]
$LAAV = 1.801AIV + 2.852$	0.90	20	[17]
$LAAV = -2.779PLI + 45.716$	0.45	50	[18]
$LAAV = 1.49AIV + 9.53$	0.79	39	[20]
$LAAV = -4.382PLI + 48.096$	0.63	40	[21]
$LAAV = 1.11AIV + 5.627$	0.48	273	[22]
$LAAV = -2.697PLI + 42.469$	0.30		
$LAAV = 0.921AIV + 3.196$*	0.81	45	[23]
$LAAV = -2.8PLI + 56.2$	0.51	8	[60]
$LAAV = 0.90AIV + 3.12$	0.68	62	[61]
$LAAV = 0.90AIV + 6.00$	0.85	18	[62]
$LAAV = -2.161PLI + 42.922$	0.56	25	The present study
$LAAV = 1.066AIV + 7.516$	0.76		
* The equation was established by reversing the original one.			

TABLE 5

Empirical relationships to predict M_{wl} as a function of w_a, M_{DE}, and γ_d

Independent variable	Test standard	Rock type	Empirical formula	R^2	Reference
M_{wl}	[32]	Limestone	$M_{wl} = 0.91M_{DE} - 1.71$	0.70	[43]
w_a			$M_{wl} = 12.18w_a - 2.89$	0.72	
M_{DE}	[32]	Limestone, granite, sandstone	$M_{wl} = 1.98M_{DE} - 14.41$*	0.66	[45]
M_{DE}	[32]	Limestone, sandstone, granite, basalt	$M_{wl} = 0.02M_{DE}^2 + 018M_{DE} + 0.92$	0.56	[46]
w_a	[36]	Limestone	$M_{wl} = 5.78w_a + 0.86$	0.65	[63]
γ_d	[35]	Various rock types	$M_{wl} = -3.436\gamma_d + 96.685$	0.59	The present study
w_a			$M_{wl} = 5.001w_a + 2.733$	0.73	
M_{DE}			$M_{wl} = 0.895M_{DE} - 6.703$	0.60	
* The equation was established by reversing the original one.					

4.2. Gene expression programming (GEP) analyses

Gene expression programming (GEP) has been used in numerous science and engineering fields to solve many geoengineering problems. The GEP is an evolutionary-based algorithm capable of producing an explicit mathematical formula linking to dependent and independent variables. The GEP was first developed by Ferreira [64]. In this section, novel applications of GEP were introduced to predict the LAAV and M_{wl}. The GeneXpro software was used to imple-

ment various GEP models. In the models, the number of chromosomes, head sizes, and gene sizes were set to 30, 8, and 3, respectively. The linking function was the addition, and root means square error (RMSE) was regarded as the fitness function. As a result of the GEP analyses, the sub-expression trees obtained from the GEP analyses are given in Fig. 5.

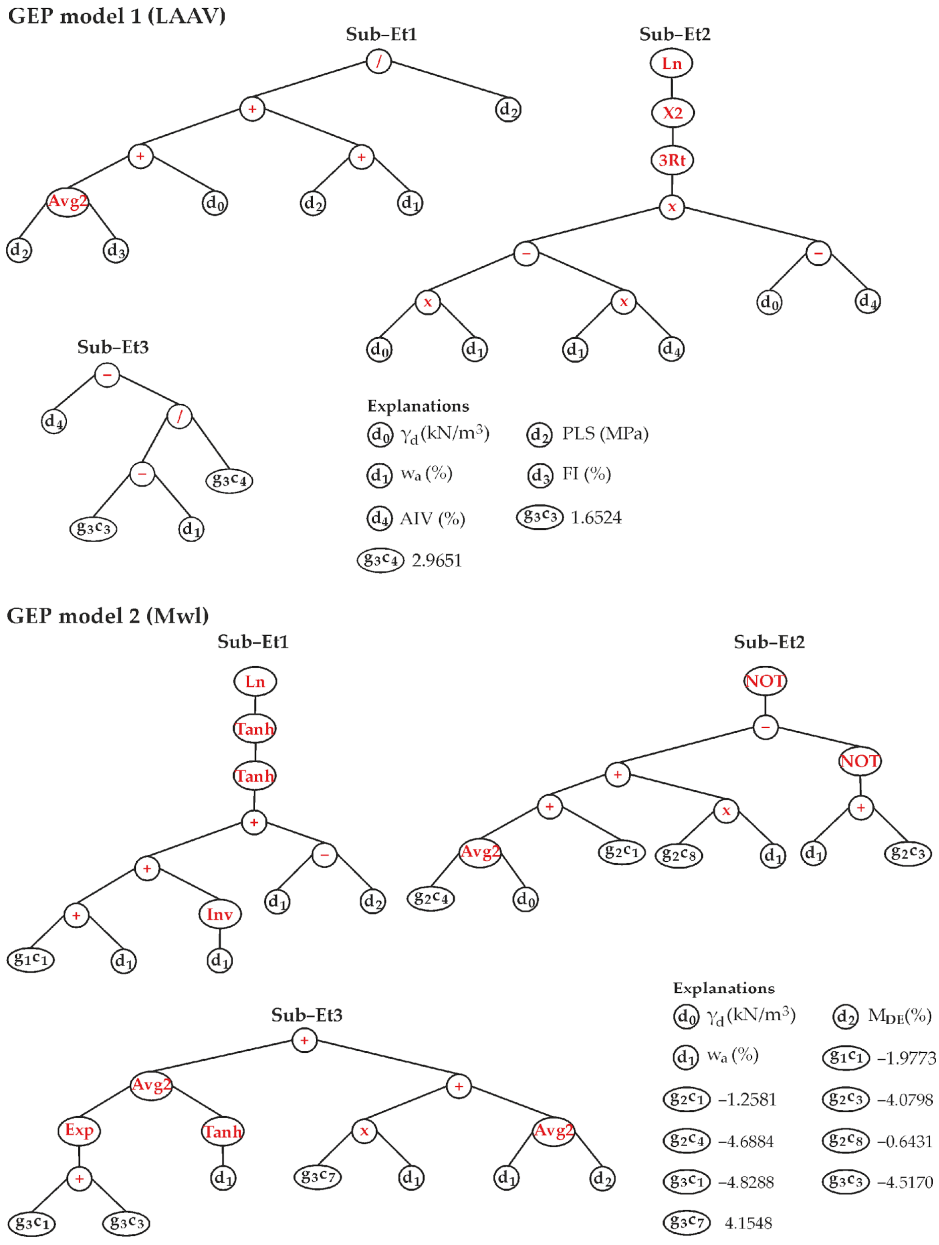

Fig. 5. Sub-expression trees for the proposed GEP model

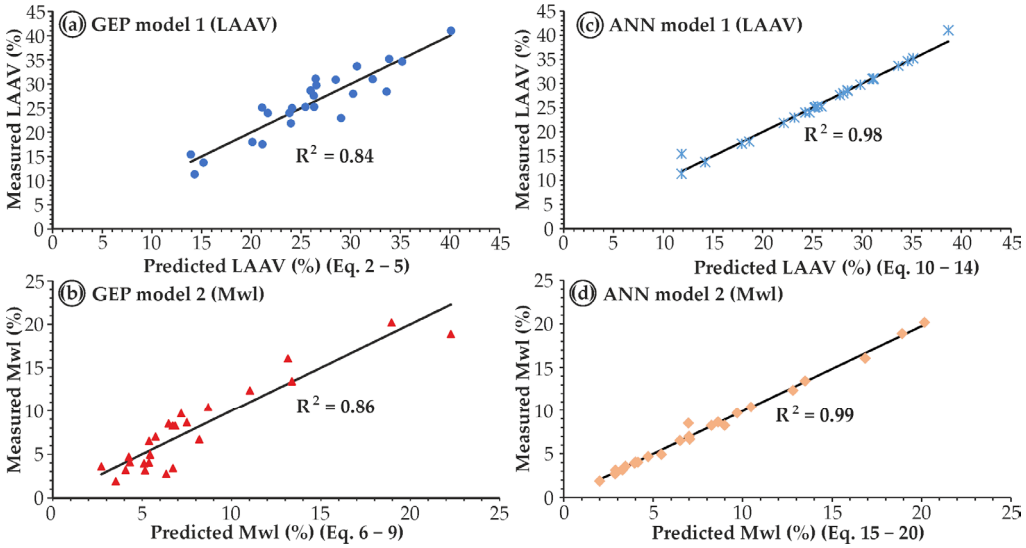

Fig. 6. Predicted and measured values obtained from the GEP and ANN analyses a) GEP model 1 for LAAV b) GEP Model 2 for M_{wl} c) ANN model 1 for LAAV d) ANN model 2 for M_{wl}

The GEP analysis results demonstrated that the proposed models have a high prediction capability with a minimum R^2 of 0.84 for the investigated dependent variables (Fig. 6a, 6b). The explicit mathematical formulae of the sub-expression trees are also presented for LAAV in Eqs 2-5 and M_{wl} in Eqs. 6-9.

$$LAAV = 1.001\sum_{i=1}^{3} x_i + 0.3075 \tag{2}$$

$$x_1 = \frac{\left(\frac{(PLS + FI)}{2} + \gamma_d\right) + (w_a + PLS)}{PLS} \tag{3}$$

$$x_2 = \ln\left(\left(\left((\gamma_d \times w_a) - (w_a \times AIV)\right) \times (\gamma_d - AIV)\right)^{2/3}\right) \tag{4}$$

$$x_3 = AIV - \frac{(1.6524 - w_a)}{2.9651} \tag{5}$$

$$M_{wl} = 0.7778\sum_{i=1}^{3} x_i + 1.5087 \tag{6}$$

$$x_1 = \ln\left(\tanh\left(\tanh\left(\left(\left(M_{DE} - 1.9773\right) + \frac{1}{w_a}\right) + \left(w_a - M_{DE}\right)\right)\right)\right) \tag{7}$$

$$x_2 = 1 - \left(\left(\frac{\left(-4.6884 + \gamma_d\right)}{2} - 1.2581 - 0.6431 w_a \right) - \left(1 - \left(w_a - 4.0798\right)\right) \right) \tag{8}$$

$$x_3 = \frac{8.734 \times 10^{-5} + \tanh\left(w_a\right)}{2} + \left(\frac{9.3096 w_a + M_{DE}}{2} \right) \tag{9}$$

4.3. Artificial neural network (ANN) analyses

Similar to the GEP models, several ANN models were also proposed to predict the LAAV and Mwl. Using the same parameters in predicting the LAAV and Mwl in the GEP analyses, various artificial neural network architectures were attempted in this study. The ANN simulations were conducted in the MATLAB environment.

Before loading the datasets into the MATLAB environment, the database (Table 3) was first pre-processed by normalising them within the range of –1 and 1 to prevent overfitting the network [65]. The datasets were divided into training (70/100), testing (15/100), and validation (15/100) datasets. Then the feed-forward backpropagation network was implemented in the training dataset. The training function was set to be Levenberg Marquardt, and the transfer function of tan sigmoid (tanh) was used in both the hidden and output layers. For LAAV prediction, the ANN architecture was defined as 5–4–1; on the other hand, for M_{wl} prediction, the ANN architecture was 3–5–1.

Based on the above explanations, the proposed ANN models are transformed into a functional mathematical form using the extracted weights and biases obtained from the ANN simulations.

The ANN-based predictive models are presented in Eqs 10-14 for LAAV and Eqs 15-20 for M_{wl}.

As for the ANN analysis results, strong correlations were obtained between the predicted and measured LAAV and Mwl values (Fig 6c, 6d). The R^2 for these models were 0.98 and 0.99, respectively. Therefore, the ANN models have a higher prediction efficiency than the proposed GEP models.

$$LAAV = 14.84 \tanh\left(\sum_{i=1}^{4} y_i - 2.0653 \right) + 26.18 \tag{10}$$

$$y_1 = -2.1359 \tanh\left(\begin{matrix} 0.6309\gamma_d + 1.7154 w_a + 0.5715 PLS + \\ +2.7978 FI - 4.6984 AIV - 2.0714 \end{matrix} \right) \tag{11}$$

$$y_2 = -0.4939 \tanh\left(\begin{matrix} 3.3992\gamma_d + 0.9167 w_a - 5.0441 PLS + \\ -6.2699 FI - 5.3027 AIV - 1.4392 \end{matrix} \right) \tag{12}$$

$$y_3 = 3.3929 \tanh\left(\begin{matrix} 0.6322\gamma_d - 2.0589 w_a - 4.1734 PLS + \\ -2.0355 FI + 3.0084 AIV - 3.6706 \end{matrix} \right) \tag{13}$$

$$y_4 = 3.1973 \tanh\left(\begin{matrix} 1.6459\gamma_d + 3.2655 w_a + 3.2215 PLS + \\ +1.5986 FI - 2.7599 AIV + 4.089 \end{matrix} \right) \tag{14}$$

$$y_4 = 3.1973 \tanh\begin{pmatrix} 1.6459\gamma_d + 3.2655 w_a + 3.2215 PLS + \\ +1.5986 FI - 2.7599 AIV + 4.089 \end{pmatrix} \quad (15)$$

$$y_1 = 3.522 \tanh\left(10.8421\gamma_d - 1.5996 w_a + 0.745 M_{DE} - 0.9823\right) \quad (16)$$

$$y_2 = 7.032 \tanh\left(3.6167\gamma_d + 3.4952 w_a - 0.5438 M_{DE} + 1.2666\right) \quad (17)$$

$$y_3 = 4.0049 \tanh\left(-10.4314\gamma_d + 0.187 w_a + 1.7675 M_{DE} + 0.8183\right) \quad (18)$$

$$y_4 = -2.8917 \tanh\left(5.0978\gamma_d + 2.3701 w_a + 6.8612 M_{DE} + 6.6141\right) \quad (19)$$

$$y_5 = -5.9888 \tanh\left(4.5912\gamma_d + 4.8939 w_a - 2.9453 M_{DE} + 0.3191\right) \quad (20)$$

4.4. Model performance

The performance of the established models was evaluated using various statistical indices such as root means squared error (RMSE), mean absolute percentage error (MAPE), and the variance accounted for (VAF). The adopted indices have been used and recommended in previous literature [65,66] to be performance indicators. The equations for calculating the above indices are listed in Eqs. 21-23.

$$RMSE = \sqrt{\frac{\sum_{i=1}^{n}\left(o_i - e_i\right)^2}{n}} \quad (21)$$

$$MAPE = \frac{1}{n}\sum_{i=1}^{n}\left|o_i - e_i\right| \quad (22)$$

$$VAF = \left(1 - \frac{\mathrm{var}\left(o_i - e_i\right)}{\mathrm{var}(o_i)}\right) \times 100 \quad (23)$$

where o_i is the observed data, e_i is the estimated data, and n is the number of observations.

The performance indicators for the proposed soft computing models are presented in Table 6. Since the proposed GEP and ANN models (Fig. 6) yield higher R^2 values than the regression models (Fig. 4), only soft computing model performances are presented in Table 6. Keep in mind that the theoretically expected R^2 value is 1, while that of VAF is 100. On the other hand, relatively successful predictive models should yield MAPE and RMSE values as small as possible. Based on this information, for the LAAV prediction, R^2, RMSE, MAPE, and VAF values of the GEP model were found to be 0.843, 2.742, 2.291, and 84.34, respectively, while their values for the ANN model were determined as 0.982, 0.945, 0.332, and 98.21, respectively. When focusing on the models estimating the M_{wl}, the R^2, RMSE, MAPE, and VAF values of the GEP model were 0.864, 1.83, 1.571, and 86.37, respectively. The values of the statistical indicators for the proposed

ANN model were 0.993, 0.413, 0.221, and 99.32. Hence, the performance of the ANN models for estimating LAAV and M_{wl} are closer to the theoretically expected R^2 and VAF values. In this direction, when comparing the statistical indicators of the GEP models with those obtained from the ANN analyses, the ANN-based models were found to have a higher prediction capability. The performance evaluation of the proposed models is also illustrated in Fig. 7, which clearly shows their prediction capability for each case.

TABLE 6

Performance evaluation of the predictive models

Model No	Dependent variable	Equation	R^2	RMSE	MAPE	VAF
GEP Models	LAAV	2	0.843	2.742	2.291	84.34
	M_{wl}	6	0.864	1.830	1.571	86.37
ANN Models	LAAV	10	0.982	0.945	0.332	98.21
	M_{wl}	15	0.993	0.413	0.221	99.32

4.5. Assessment of the investigated rocks for bituminous paving mixtures based on the proposed soft computing models

The soft computing tools (i.e., GEP and ANN) utilised in this study provide practical knowledge about estimating the LAAV and M_{wl} values of the investigated rocks. For a deeper investigation of the suitability and long-term usability of the investigated rocks, the measured and predicted LAAV and M_{wl} values were considered concerning the technical requirements of ASTM D692 / D692M [54]. Prior to this evaluation, it should be mentioned that based on the regression analysis (Fig. 4), the LAAV can be declared as a function of AIV, MDE, and PLS to some extent. On the other hand, the M_{wl} is associated mainly with the w_a of the investigated rocks.

Using such rock properties, strong predictive models were established based on the GEP and ANN analyses. Since the LAAV and M_{wl} are critical parameters, especially for road and pavement design studies, they were evaluated using high-precision measuring tools or techniques. For assessing the rock aggregate quality, these parameters (i.e., LAAV and M_{wl}) were emphasised and highlighted by Köken et al. [67]. In that study, rock weathering was declared a critical phenomenon for rock quality control processes. Since progressive rock weathering decreases the overall rock quality, only unweathered rock materials were considered and used in the present study. Therefore, their weathering trends were not evaluated. It is, however, required to have quantitative results on their weathering trends using rock weathering indices or ageing tests for further studies. Notably, the w_a is a critical variable for bituminous paving mixtures. It is also necessary to be considered since asphalt absorption of rock aggregates in bituminous paving mixtures is associated with the w_a of rocks [68, 69].

Coming back to the predicted LAAV and M_{wl} values, when comparing the LAAV and M_{wl} values obtained from the GEP and ANN models, it can be claimed that the predictions of the GEP models are sensitive to various rock types. On the other hand, the ANN model seems to be more stable and provides more consistent LAAV and M_{wl} values (Fig. 7).

Therefore, it is recommended that the ANN-based models (Eqs 10, 15) could be reliably used to estimate LAAV and M_{wl} for the investigated rocks. Nevertheless, the proposed GEP models should be improved by adding new rock types and/or input parameters.

Anyhow, this work can be declared a case study showing the applicability of GEP and ANN methodologies for the evaluation of LAAV and Mwl of some aggregates from Turkey. Hence, the number of samples should be increased to obtain general inferences in further studies.

The technical requirements of ASTM D692/D692M [54] for bituminous paving mixtures were also plotted in Fig. 7. In this regard, only one rock type (R7) seems to be unsuitable for use in bituminous paving mixtures when considering its LAAV value.

Nonetheless, R7 and R13 are critical rock types in their use based on their M_{wl} values. R7 was a porous limestone, and R13 was defined as andesite in lithology. Based on the sampling frequency limit proposed by Phillips [45] (i.e., $M_{wl} \leq 10\%$), R14-16 and R22 should be considered/tested every 18-24 months in terms of their M_{wl} values for their long-term stability. The lithology of these rocks (R14-R16 and R22) are andesite and granite. These are practically known as unsuitable rock types for long-term use in paving mixtures, although their technical requirements are eligible for initial use. R4 can also be added to this group of rocks.

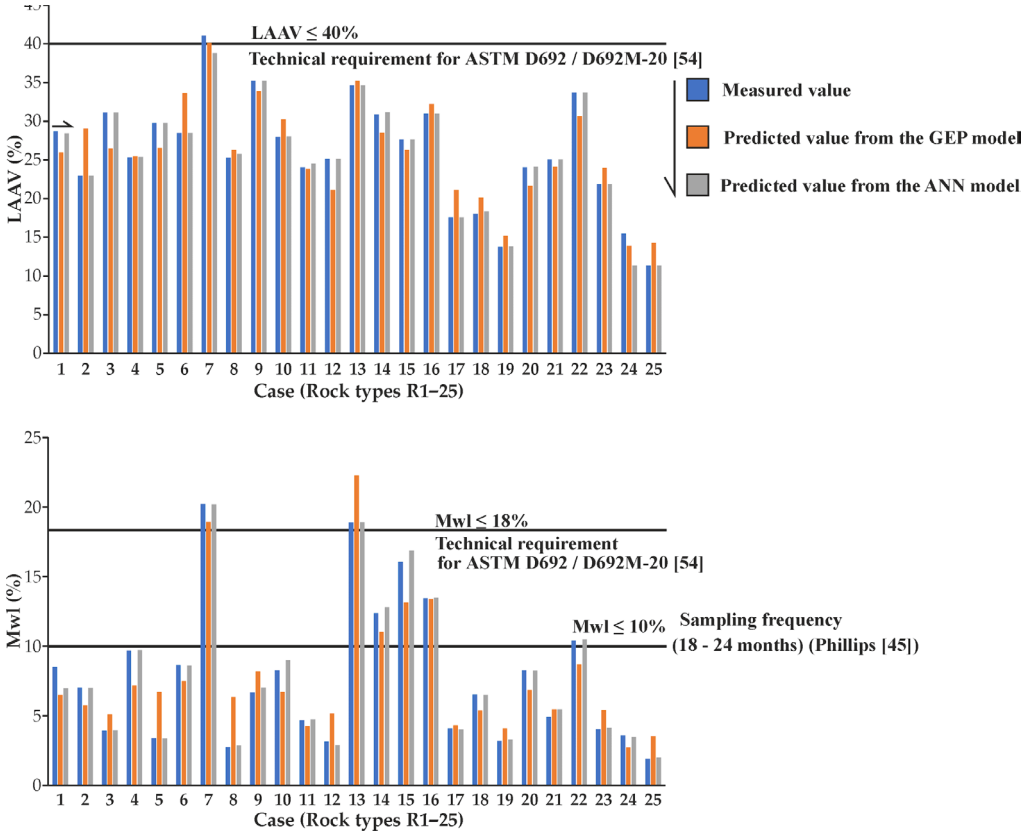

Fig. 7. Comparison of the proposed models for each case

5. Conclusions

This study evaluated the LAAV and M_{wl} of 25 different rock types in NW Turkey using regression analyses and soft computing methods such as GEP and ANN. The above rock aggregate properties are critical parameters because they provide quantitative knowledge on aggregate quality assessment in numerous engineering applications.

However, their laboratory experiments are costly and time-consuming. Hence, it is required to develop robust models that can minimise the experimental time and cost of these critical rock aggregate parameters. To achieve the aim of this study, various laboratory tests were conducted to determine the γ_d, w_a, PLS, AIV, LAAV, $M_{DE,}$ and M_{wl} in accordance with the ISRM, BS, TS and EN standards. Then, the obtained laboratory results were transformed into a comprehensive database and used in developing the proposed GEP (Eqs 2, 6) and ANN (Eqs 10, 15) models. Before developing the GEP and ANN models, regression analyses were first conducted to reveal statistically correlative parameters for the evaluation of LAAV and M_{wl}. Then, soft computing analyses were carried out, considering the obtained correlative parameters. Furthermore, the suitability of the assessed rock types for use in bituminous paving mixtures is also investigated.

The main conclusions obtained from the present study can be drawn as follows:

- The prediction capability of the GEP and ANN models is closer to the laboratory-measured values than the regression model predictions. Based on the performance evaluation of the models, the proposed ANN models outperformed the other models established in this study. Therefore, it is recommended that the ANN-based predictive models be used to estimate the LAAV and M_{wl} of the investigated rocks.
- Most of the investigated rocks (except R_7) are suitable for use in bituminous paving mixtures. Rock types of $R_{14–16}$ and R_{22} should be further investigated for their long-term suitability in bituminous paving mixtures.
- Explicit mathematical formulations of the proposed GEP and ANN models were introduced in this study. These models can easily be implemented by coding them in any computer programming language, paving the way for assessing rock aggregate quality. However, the GEP models should be improved by attempting other fitness functions and/or input parameters.

Acknowledgment

The author is indebted to Abiodun Ismail Lawal (Federal University of Technology, Akure) for his valuable help in soft computing analyses.

References

[1] USGS, Mineral Industry Surveys: Crushed stone and sand and gravel in the fourth quarter 2020, (2021). https://www.usgs.gov/centers/nmic

[2] A.A. Al-Harthi, A field index to determine the strength characteristics of crushed aggregate. Bulletin of Engineering Geology and the Environment **60**, 193-200 (2001). DOI: https://doi.org/10.1007/s100640100107

[3] P.S. Kandhal, F. Parker, Aggregate tests related to asphalt concrete performance in pavements. Final Report (NO: 405) Transportation Research Board. Washington, (1998), USA.

[4] C. Mitchell, Construction aggregates: evaluation and specification. Third International Forum for Industrial Rocks & Mining conference & exhibition, Fujairah, United Arab Emirates, (2015).

[5] E. Erichsen, A. Ulvik, K. Sævik, Mechanical degradation of aggregate by the Los Angeles-, the Micro-Deval- and the Nordic Test Methods. Rock Mechanics and Rock Engineering **44**, 333-337 (2011). DOI: https://doi.org/10.1007/s00603-011-0140-y

[6] Y. Qian, H. Boler, M. Moaveni, E. Tutumluer, Y.M.A. Hashash, J. Ghaboussi, Characterizing ballast degradation through Los Angeles abrasion test and image analysis. Transportation Research Record **2448** (1), 142-151 (2014). DOI: https://doi.org/10.3141/2448-17

[7] A. Török, Los Angeles and Micro-Deval Values of Volcanic Rocks and Their Use as Aggregates, Examples from Hungary. In: Lollino G., Manconi A., Guzzetti F., Culshaw M., Bobrowsky P., Luino F. (eds) Engineering Geology for Society and Territory **5**, 115-118 (2015). DOI: https://doi.org/10.1007/978-3-319-09048-1_23

[8] J. Wu, Y. Hou, L. Wang, M. Guo, L. Meng, H. Xiong, Analysis of coarse aggregate performance based on the modified Micro Deval abrasion test. International Journal of Pavement Research and Technology **11** (2) 185-194 (2018). DOI: https://doi.org/10.1016/j.ijprt.2017.10.007

[9] E. Köken, A. Özarslan, G. Bacak, An experimental investigation on the durability of railway ballast material by magnesium sulfate soundness. Granular Matter **20**, 29 (2018). DOI: https://doi.org/10.1007/s10035-018-0804-3

[10] E.T. Tunc, K.E. Alyamac, Determination of the relationship between the Los Angeles abrasion values of aggregates and concrete strength using the Response Surface Methodology. Construction, and Building Materials **260** (10), 11985 (2020). DOI: https://doi.org/10.1016/j.conbuildmat.2020.119850

[11] V. Hofer, H. Bach, C. Latal, A.C. Neubauer, Impact of geometric and petrographic characteristics on the variability of LA test values for railway ballast. Mathematical Geosciences **45**, 727-752 (2013). DOI: https://doi.org/10.1007/s11004-013-9472-3

[12] S. Kahraman, O.Y. Toraman, Predicting Los Angeles abrasion loss of rock aggregates from crushability index. Bulletin of Materials Science **31**, 173-177 (2008). DOI: https://doi.org/10.1007/s12034-008-0030-4

[13] R. Ajalloeian, M. Kamani, An investigation of the relationship between Los Angeles abrasion loss and rock texture for carbonate aggregates. Bulletin of Engineering Geology and the Environment **78**, 1555-1563 (2019). DOI: https://doi.org/10.1007/s10064-017-1209-y

[14] S. Kahraman, O. Gunaydin, Empirical methods to predict the abrasion resistance of rock aggregates. Bulletin of Engineering Geology and the Environment **66**, 449-455 (2007). DOI: https://doi.org/10.1007/s10064-007-0093-2

[15] I. Ugur, S. Demirdag, H. Yavuz, Effect of rock properties on the Los Angeles abrasion and impact test characteristics of the aggregates. Materials Characterization **61** (1), 90-96 (2010). DOI: https://doi.org/10.1016/j.matchar.2009.10.014

[16] Y. Ozcelik, Predicting Los Angeles abrasion of rocks from some physical and mechanical properties. Scientific Research and Essays, **6** (7), 1612-1619 (2011).

[17] M. Palassi, A. Danesh, Relationships Between Abrasion/Degradation of Aggregate Evaluated from Various Tests and the Effect of Saturation. Rock Mechanics and Rock Engineering **49**, 2937-2943 (2016). DOI: https://doi.org/10.1007/s00603-015-0869-9

[18] L.O. Afolagboye, A.O. Talabi, C.A. Oyelami, The use of index tests to determine the mechanical properties of crushed aggregates from Precambrian basement complex rocks, Ado-Ekiti, SW Nigeria. Journal of African Earth Sciences **129**, 659-667 (2017). DOI: https://doi.org/10.1016/j.jafrearsci.2017.02.013

[19] M. Ahmad, M.K. Ansari, L.K. Sharma, R. Singh, T.N. Singh, Correlation between Strength and Durability Indices of Rocks – Soft Computing Approach. Procedia Engineering **191**, 458-466 (2017). DOI: https://doi.org/10.1016/j.proeng.2017.05.204

[20] A. Teymen, Estimation of Los Angeles abrasion resistance of igneous rocks from mechanical aggregate properties. Bulletin of Engineering Geology and the Environment **78**, 837-846 (2019). DOI: https://doi.org/10.1007/s10064-017-1134-0

[21] M. Kamani, R. Ajalloeian, Evaluation of the mechanical degradation of carbonate aggregate by rock strength tests. Journal of Rock Mechanics and Geotechnical Engineering **11** (1), 121-134 (2019). DOI: https://doi.org/10.1016/j.jrmge.2018.05.007

[22] M.K. Esfahani, M. Kamani, R. Ajalloeian, An investigation of the general relationships between abrasion resistance of aggregates and rock aggregate properties. Bulletin of Engineering Geology and the Environment **78**, 3959-3968 (2019). DOI: https://doi.org/10.1007/s10064-018-1366-7

[23] M. Asadi, A. Taghavi Ghalesari, S. Kumar, Machine learning techniques for estimation of Los Angeles abrasion value of rock aggregates. European Journal of Environmental and Civil Engineering, (2019). DOI: https://doi.org/10.1080/19648189.2019.1690585

[24] U. Åkesson, J.E. Lindqvist, M. Göransson, J. Stigh, Relationship between texture and mechanical properties of granites, central Sweden, by use of image-analyzing techniques. Bulletin of Engineering Geology and the Environment **60**, 277-284 (2001). DOI: https://doi.org/10.1007/s100640100105

[25] F. Röthlisberger, J. Däppen, E. Kurzen, E. Würsch, Los Angeles Prüfung für Gleisschotter – Aussagekraft und Folgerung. Eisenbahntechnische Rundschau **54** (6), 355-361 (2005).

[26] F.N. Okonta, Relationships Between Abrasion Index and Shape Properties of Progressively Abraded Dolerite Railway Ballasts. Rock Mechanics and Rock Engineering **47**, 1335-1344 (23014). DOI: https://doi.org/10.1007/s00603-013-0474-8

[27] M. Risnen, Relationships between texture and mechanical properties of hybrid rocks from the Jaala–Iitti complex, southeastern Finland. Engineering Geology **74** (3-4), 197-211 (2004). DOI: https://doi.org/10.1016/j.enggeo.2004.03.009

[28] H. Liu, S. Kou, P.A. Lindqvist, Microscope rock texture characterization and simulation of rock aggregate properties. Technical report SGU project 60-1362/2004, Geological Survey of Sweden, (2005).

[29] J. Stålheim, Comparative study of established test methods for aggregate strength and durability of Archean rocks from Botswana. Uppsala Universitet, Report No: W13044, (2014).

[30] I.W.T.P Dayarathna, U.G.A. Puswewala, A.M.K.B. Abeysinghe, L.P.S. Rohitha, Relationship between Los Angeles Abrasion Value and Mineral Content of Metamorphic Rocks. International Symposium on Earth Resources Management and Environment (ISERME 2017), Wadduwa, Sri Lanka, (2017).

[31] V. Hofer, H. Bach, Statistical monitoring for continual quality control of railway ballast. Expert Systems with Applications **42** (22), 8557-8572 (2015). DOI: https://doi.org/10.1016/j.eswa.2015.07.011

[32] AASHTO T104, Standard Method of Test for Soundness of Aggregate by Use of Sodium Sulfate or Magnesium Sulfate. American Association of State Highway and Transportation Officials, (2003).

[33] TS EN 1367-1, Tests for thermal and weathering properties of aggregates – Part 1: Determination of resistance to freezing and thawing. Turkish Standards Institution, Ankara, (2008).

[34] ASTM D6035/D6035M-13, Standard Test Method for Determining the Effect of Freeze-Thaw on Hydraulic Conductivity of Compacted or Intact Soil Specimens Using a Flexible Wall Permeameter. ASTM International, West Conshohocken, PA, (2013).

[35] TS EN 1367-2, Tests for thermal and weathering properties of aggregates – Part 2: Magnesium sulfate test. Turkish Standards Institution, Ankara, (2010).

[36] ASTM C88/C88M-18, Standard Test Method for Soundness of Aggregates by Use of Sodium Sulfate or Magnesium Sulfate. ASTM International, West Conshohocken, PA, (2018).

[37] S. Geving, J.V. Thue, Fuktibygninger (Moisture in buildings, in Norwegian). NBI handbook 50. Oslo: Norwegian Building Research Institute, (2002).

[38] J. Ruedrich, S. Siegesmund, Salt and ice crystallisation in porous sandstones. Environmental Geology **52**, 225-249 (2007). DOI: https://doi.org/10.1007/s00254-006-0585-6

[39] H. Ouacha, A. Ben-Moussa, J. Simao, The salt crystallization weathering of building rocks of the archaeological sites calcarenites of north-western morocco (lixus, banasa and thamusida). European Scientific Journal **9** (18) 282-290 (2013).

[40] H.C. Helgeson, J.M. Delany, H.W. Nesbitt et al., Summary and critique of the thermodynamic properties of rock-forming minerals. American Journal of Science 278A, 1-229 (1978).

[41] G.D. Price, N.L. Ross, The stability of minerals; The mineralogical society series 3. Kluwer Academic Publishers, ISBN: 0-412-44150-0, (1992).

[42] B. Vásárhelyi, P. Ván, Influence of water content on the strength of rock. Engineering Geology **84** (1-2), 70-74 (2006). DOI: https://doi.org/10.1016/j.enggeo.2005.11.011

[43] P.W. Jayawickrama, S. Hossain, A.R. Hoare, Long-term Research on Bituminous Coarse Aggregate: Use of Micro-deval Test for Project Level Aggregate Quality Control. Texas Technical University, Research Report, Report No: FHWA/TX-06/0-1707-9, 89 pp, (2007).

[44] C.A. Rogers, M.L. Bailey, B. Price, Micro-Deval Test for Evaluating the Quality of Fine Aggregate for Concrete and Asphalt. Transportation Research Record **1301**, 68-76 (1991).

[45] F.W. Phillips, Comparative analysis between the magnesium sulfate soundness and Micro-Deval tests in the evaluation of bituminous aggregates. Master's Thesis, Texas Tech University, Lubbock, TX, USA, (2000).

[46] D.W. Fowler, J.J. Allen, A. Lange, P. Range, The Prediction of Coarse Aggregate Performance by Micro-Deval and Other Aggregate Tests. Research Report in International Center for aggregates research, (ICAR), Report No: ICAR 507-1F, (2006).

[47] ISRM, The complete ISRM suggested methods for rock characterization, testing and monitoring: 1974-2006. In: Ulusay R, Hudson JA(eds) Suggested methods prepared by the commission on testing methods. Int. Soc. Rock Mech. (ISRM), Ankara, Turkey, (2007).

[48] BS 812-112, British standard: Testing aggregates, method for determination of aggregate impact value (AIV), (1990).

[49] TS EN 1097-2, Tests for mechanical and physical properties of aggregates – Part 2: Methods for the determination of resistance to fragmentation. Turkish Standards Institution, Ankara, (2010).

[50] TS EN 1097-1, Tests for mechanical and physical properties of aggregates – Part 1: Determination of the resistance to wear (micro-Deval). Turkish Standards Institution, Ankara, (2011).

[51] M.L. Larrea, S.M. Castro, E.A. Bjerg, A software solution for point counting. Petrographic thin section analysis as a case study. Arab. J. Geosci. **7**, 2981-2989 (2014). DOI: https://doi.org/10.1007/s12517-013-1032-0

[52] BS EN 933-3, Tests for geometrical properties of aggregates; Determination of particle shape. Flakiness Index, British Standards Institution, (2012).

[53] E. Broch, J.A. Franklin, The Point-Load Strength Test. International Journal of Rock Mechanics and Mining Sciences **9** (6), 669-697 (1972). DOI: https://doi.org/10.1016/0148-9062(72)90030-7

[54] ASTM D692/D692M-20, Standard Specification for Coarse Aggregate for Asphalt Paving Mixtures. ASTM International, West Conshohocken, PA, (2020).

[55] I. Rigopoulos, B. Tsikouras, P. Pomonis K. Hatzipanagiotou, Determination of the interrelations between the engineering parameters of construction aggregates from ophiolite complexes of Greece using factor analysis. Constr. Build. Mater. **49**, 747-757 (2013). DOI: https://doi.org/10.1016/j.conbuildmat.2013.08.065

[56] S. Adomako, C.J. Engelsen, R.T. Thorstensen, D.A. Barbieri, Review of the relationship between aggregates geology and Los Angeles and micro-Deval tests. Bull Eng Geol Environ. **80**, 1963-1980 (2021).
DOI: https://doi.org/10.1007/s10064-020-02097-y

[57] J.M.R. Fernlund, 3-D image analysis size and shape method applied to the evaluation of the Los Angeles test. Engineering Geology. **77** (1-2), 57-67 (2005). DOI: https://doi.org/10.1016/j.enggeo.2004.08.002

[58] P. Strzałkowski, U. Kaźmierczak, Wear and Fragmentation Resistance of Mineral Aggregates – A Review of Micro-Deval and Los Angeles Tests. Materials **14** (18), 5456 (2021).
DOI: https://doi.org/10.3390/ma14185456

[59] E. Erichsen, A. Ulvik, K. Sævik, Mechanical Degradation of Aggregate by the Los Angeles-, the Micro-Deval- and the Nordic Test Methods. Rock Mech. Rock Eng. **44**, 333 (2011).
DOI: https://doi.org/10.1007/s00603-011-0140-y

[60] T.Y. Irfan, Aggregate properties and resources of granitic rocks for use in concrete in Hong Kong. Quarterly Journal of Engineering Geology **27**, 25-38 (1994). DOI: https://doi.org/10.1144/GSL.QJEGH.1994.027.P1.05

[61] A.A Al Harthi, Y.E. Abo Saada, Wadi natural aggregates in western Saudi Arabia for use in concrete. Bulletin of the International Association of Engineering Geology – Bulletin de l'Association Internationale de Géologie de l'Ingénieur **55**, 27-37 (1997). DOI: https://doi.org/10.1007/BF02635406

[62] G. Koukis, N. Sabatakakis, A. Spyropoulos, Resistance variation of low-quality aggregates. Bulletin of Engineering Geology and the Environment. **66**, 457-466 (2007). DOI: https://doi.org/10.1007/s10064-007-0098-x

[63] P.W. Jayawickrama, Limitations on the Use of Aggregate Sulfate Soundness for the Prediction of Field Performance of Hmac and Seal Coat Pavement Surfaces, Texasn Technical University, Texas Department of Transportation, Report No: 118D91-1929, 88 pp, (1992).

[64] C. Ferreira, Gene expression programming: A new adaptive algorithm for solving problems. Complex Systems **13** (2), 87-129 (2001).

[65] A.I. Lawal, M.A. Idris, An artificial neural network-based mathematical model for the prediction of blast-induced ground vibrations. International Journal of Environmental Studies **77** (2), 318-334 (2020). DOI: https://doi.org/10.1080/00207233.2019.1662186

[66] M. Onifade, A.I. Lawal, E.A. Aladejare, S. Bada, M.A. Idris, Prediction of gross calorific value of solid fuels from their proximate analysis using soft computing and regression analysis. International Journal of Coal Preparation and Utilization, (2019). DOI: https://doi.org/10.1080/19392699.2019.1695605

[67] E. Köken, S. Top, A. Özarslan, Assessment of Rock Aggregate Quality Through the Analytic Hierarchy Process (AHP). Geotechnical and Geological Engineering **38**, 5075-5096 (2020). DOI: https://doi.org/10.1007/s10706-020-01349-8

[68] D.Y. Lee, Absorption of asphalt into porous aggregates. Strategic Highway Res. Prog. Report (No: SHRP-A/UIR 90–009, Washington, (1990).

[69] A.R. Tarrer, V. Wagh, The effect of physical and chemical characteristics of the aggregate in bonding. Strategic Highway Res. Prog. Report No: SHRP-A/UIR 97–507, Washington, (1991).